TG Wave Autoresonant Control of Plasma Temperature

A.A. Kabantsev [a)] and C.F. Driscoll

Department of Physics, University of California at San Diego, La Jolla, CA 92093-0354, USA
[a)] Corresponding author: akabantsev@ucsd.edu

Abstract. The thermal correction term in the Trivelpiece-Gould (*TG*) wave's frequency has been used to accurately control the temperature of electron plasma, by applying a swept-frequency continuous drive autoresonantly locked in balance with the cyclotron cooling. The electron temperature can be either "pegged" at a desired value (by constant drive frequency); or varied cyclically (following the tailored frequency course), with rates limited by the cooling time (on the way down) and by chosen drive amplitude (on the way up).

INTRODUCTION

We describe sensitive temperature measurements obtained from the standard diocotron mode, and robust temperature control obtained from autoresonant drive of Trivelpiece-Gould modes. These electron plasma experiments were done on the CamV apparatus at magnetic field $B = 1.2$ Tesla. The description and typical plasma and trap parameters may be found elsewhere [1-3].

Various techniques are used to continuously monitor the plasma temperature. Measurements of the frequencies of the plasma modes is an attractive way of accomplishing this since the frequencies can be measured with great precision, and an entire time history can be reconstructed in one experimental cycle. In some experiments [4-6], the frequency shifts of the quadrupole mode in spheroidal nonneutral plasmas have been used to calculate the magnitude of the temperature change. However, our plasmas have high aspect ratios, and they are not confined in a harmonic potential. This makes the modes very difficult to interpret for the temperature measurements. In other experiments, thermally-excited fluctuations in axial motion of plasma particles have been used as a basis for temperature diagnostics [7, 8]. This completely passive diagnostics has many appealing features, but, due to the transient nature of fluctuating modes, their accuracy of frequency measurements is not high enough to serve in our case as a definitive diagnostic tool.

Here we utilize the frequency of the basic diocotron mode as a sensitive probe of plasma temperature. The fundamental $k_z = 0,\ l_\theta = 1$ diocotron mode is neutrally stable (neglecting its interaction with the wall), so a single mode can persist during the entire plasma evolution cycle. The finite length diocotron mode has a frequency shift arising due to the thermal pressure of plasma column on the ends [9]:

$$f_d(t) = \frac{ceN}{\pi B R_W^2}\left\{1 + \frac{R_W}{L_p}\left[1.20\left(\frac{1}{4} + \ln\frac{R_W}{R(t)} + \frac{T(t)}{e^2 N}\right) - 0.671\right]\right\}\left[1 + \sigma\frac{D^2}{R_W^2}\right]. \tag{1}$$

Here, if we assume that the plasma line density $N \equiv \int_0^{R_W} 2\pi r dr\, n(r)$ is constant, and the mode amplitude (displacement) D is constant, then temporal frequency changes will be only due to changes in plasma temperature $T(t)$ or characteristic plasma radius $R(t)$. For typical parameters, $e^2 N \approx 10$ eV and $L_p/R_W \approx 14$ (the aspect ratio), a 1 eV temperature change results in about 1% change of the diocotron frequency $f_d(t)$, so the measurement accuracy of $\Delta f_d/f_d \sim 10^{-4}$ allows one to assess temperature variations down to the room value of 0.03 eV. We have also used destructive temperature diagnostics based on measuring the rate at which electrons evaporate out of a confining potential well as the well barrier is lowered [10] to verify and to calibrate the diocotron frequency shifts versus plasma temperature.

TEMPERATURE CONTROL TECHNIQUE

The Trivelpiece-Gould (*TG*) plasma wave frequencies also have a thermal correction term [11], but the important difference here is that the *TG* waves are typically strongly damped, and thus produce plasma heating.

This temperature dependence of the *TG* wave frequency can be used to actively control the temperature of electron plasmas, using a swept-frequency autoresonant drive. A simple cartoon of this process is shown in Fig. 1. Here, the driven *TG* waves heat the plasma autoresonantly, in balance with the intrinsic cyclotron cooling at a typical rate of $\tau_c^{-1} \approx (B^2/3.9)\ \mathrm{sec}^{-1}$, where B is in Teslas. In a Penning-Malmberg trap with long aspect ratio, the $k_z = 1,2,3,\ldots, l_\theta = 0$ *TG* wave frequencies are temperature-dependent, as

$$f_{TG}(T) \approx f_{TG}(0) * \left\{1 + \frac{3}{4\ln R_W/R}\frac{T}{e^2 N}\right\} \equiv f_{TG}(0) * \{1 + \varepsilon T\}, \tag{2}$$

where $\varepsilon \ll 1\ \mathrm{eV}^{-1}$. A frequency sweep $f_{dr}(t)$ through a *TG* mode resonance exhibits quite a narrow and tall Lorentzian absorption response $\mathcal{L}(f_{dr}; f_{TG}, \gamma_{TG})$ with a typical resonance width of $\gamma_{TG}(T) {\sim} 10^{-3} f_{TG}$. A continuously applied drive then produces plasma heating power $P_h(f_{dr}) \propto \gamma_{TG} A_{dr}^2 \mathcal{L}(f_{dr}; f_{TG}, \gamma_{TG})$, which can exactly balance the cyclotron cooling power $P_c(T) \propto T/\tau_c$. In Fig. 1, the tall (blue) peak is P_h at 0.50 eV, and the low (green) peak is P_h at 0.52 eV. The straight (red) line is the nearly constant P_c. With sufficient drive power, there are 2 balance points where $P_h = P_c$.

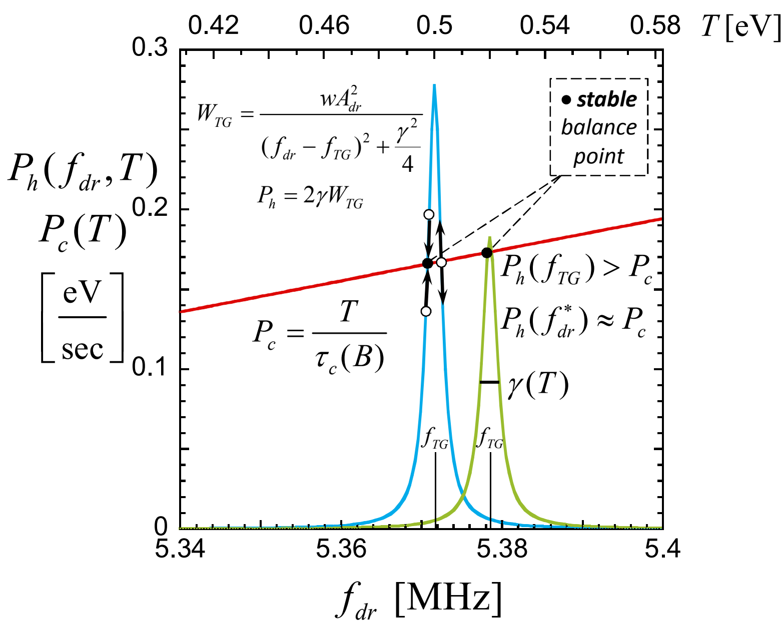

FIGURE 1. Cartoon of the autoresonant frequency–temperature locking. The top X-axis shows plasma temperatures matching to the resonant $k_z = 3$ *TG* mode frequency $f_{TG3}(T)$. When $P_h(f_{TG}) > P_c(T)$, there is the stable thermal balance point to the left of the $P_h(f_{dr}; T)$ resonance peak. A slow sweep of the drive frequency $f_{dr}(t)$ keeps the thermal balance locked by properly adjusting the plasma temperature according to the given frequency change.

The balance point is autoresonantly *stable* (i.e., the plasma temperature is locked to the drive frequency) when $f_{dr} = f_{dr}^* \approx f_{TG}(T) - \gamma_{TG}$. If the temperature increases, then $f_{TG}(T)$ also increases and f_{dr} gets further away from the resonance, so the heating power decreases and $T(t)$ settles back to the balance point. If the temperature $T(t)$ decreases, then $f_{TG}(T)$ also decreases and f_{dr} gets closer to the *TG* mode resonance, so the heating power goes up, and T settles back to the balance point again. The second power-balance point at $f_{dr} \approx f_{TG}(T) + \gamma_{TG}$ is obviously *unstable*.

Now, if one starts a slow sweep of the drive frequency $f_{dr}(t)$ from some value located well below a *TG* mode resonance, then no (significant) heating is happening until the frequency gets close to $f_{dr} \approx f_{TG}(T) - \gamma_{TG}$. At that point the drive power couples efficiently to the damped *TG* mode, so the heating power overcomes the cyclotron cooling, and the plasma temperature rises in order to keep the thermal balance. Thus, after the initial lock-in is established, the plasma temperature follows the drive frequency upswing until the extreme balance point where the increasing cooling power and the (fast rising) mode damping rate collaborate to match at the maximum heating point $P_c(T) = P_h(f_{TG})$. After that point the power balance is lost, and the plasma starts to cool down until the climbing drive frequency reaches the next wave number TG resonance. Then this frequency–locked heating cycle repeats itself again and again.

When the drive frequency sweep changes direction and starts going down, there are two possible outcomes for the plasma temperature evolution. If the drive frequency goes down rather slow in comparison to the cyclotron cooling rate, then the thermal balance stays frequency locked, and the plasma temperature follows the drive frequency path. If the drive frequency goes down faster than the cooling rate, then the frequency–locked thermal balance is lost, the plasma temperature gets detached from the drive frequency and goes into the cyclotron cooling phase.

RESULTS AND DISCUSSIONS

Figure 2 shows the relative changes of diocotron frequency (the left Y-axis) and the corresponding plasma temperature (the right Y-axis), taken during a linear sweep of the drive frequency (shown on the top X-axis) through $k_z = 3$ and 4 TG modes. Here, the room temperature limits are $f_{TG3} \approx 5.6$ MHz and $f_{TG4} \approx 7.3$ MHz. When the drive power is applied to the trap's midplane, then only even TG modes (here, $k_z = 4$) show the autoresonant frequency–temperature locking. When the drive power is applied to the trap's end, then both even and odd TG modes (here, $k_z = 3$ and 4) show the autoresonantly locked to the drive frequency heating. Upon reaching the temperatures of about 1.5 eV (depending on the power of the drive) the thermal balance is lost, and the plasma temperature goes into the cyclotron cooling phase until the next allowed k_z TG mode frequency locking. Linear drive frequency upward sweep from 1 to 15 MHz shows all $k_z = 1,2,\dots 7$ frequency–temperature locks admissible for the given plasma column geometry. The frequency drive has typical amplitude of 50 mV applied to a small angular sector of the cylindrical wall. At these conditions, the non–resonant heating of the plasma is negligible.

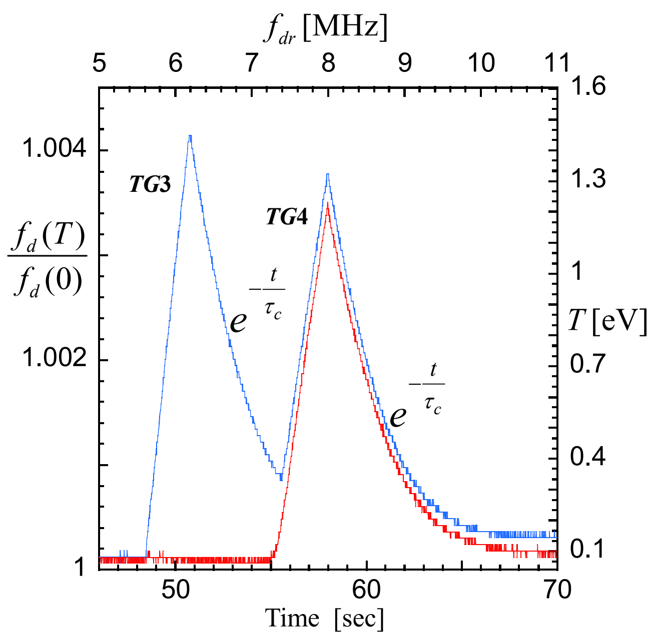

FIGURE 2. Plasma temperature (the right Y-axis) and diocotron frequency (the left Y-axis) evolutions during the drive frequency $f_{dr}(t)$ upward sweep at 0.5MHz/sec rate through the $TG3$ and $TG4$ plasma modes frequency domain.

Figure 3 shows the diocotron frequency and corresponding plasma temperature taken during linear scans from 5.4 MHz → 6.4 MHz (i.e., around $TG3$), with the scan duration varying from 1 sec to 15 sec. As the drive frequency sweep time varies, the resulting plasma temperatures follow the frequency sweeps after the initial frequency–temperature locking has occurred. The somewhat faster initial growth of the plasma temperature visible at slow sweeps is due to the initial heating in transition to the stable balance point (see Fig. 1). Once the drive frequency is turned off, the plasma temperature goes into the cyclotron cooling phase characterized by an exponential rate e^{-t/τ_c}.

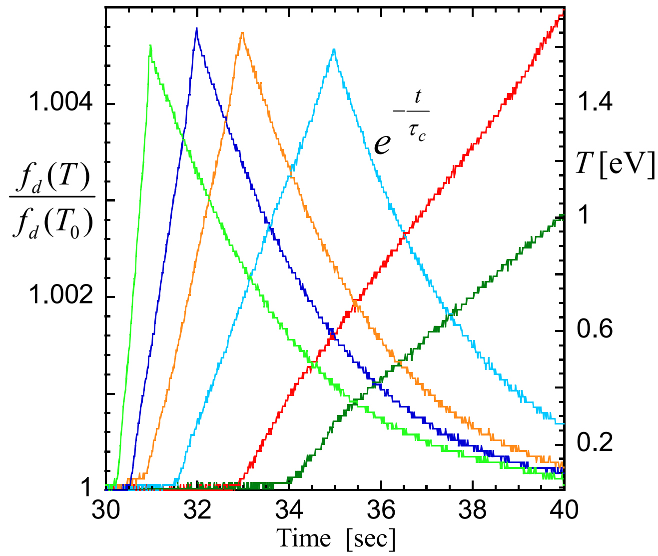

FIGURE 3. Plasma temperature and diocotron frequency evolutions during the drive frequency $f_{dr}(t)$ sweep from 5.4 MHz to 6.4 MHz (the *TG*3 mode frequency domain) with various rates $1\text{MHz}/\tau$, where $\tau = 1,2,3,5,10,$ and 15 sec.

Figure 4 shows results of application of a slow ($f_M = 0.04$ Hz) sinusoidal baseband modulation of the drive frequency around the $k_z = 3$ *TG* mode frequency. Here we characterize the drive frequency as $f_{dr}(t) = f_i + 2f_\Delta \sin^2 \pi f_M t$, where $f_i = 5.5$ MHz is the initial (base) drive frequency, $2f_\Delta$ is the variable frequency deviation band, and f_M is the drive frequency modulation rate. After an initial exponential drop (post injection cyclotron cooling) the plasma temperature shows sinusoidal oscillations locked to the corresponding drive frequency modulations.

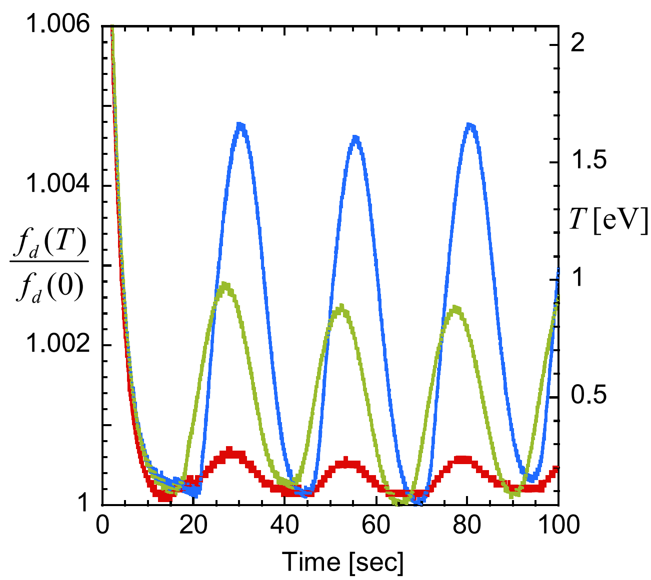

FIGURE 4. Plasma temperature and diocotron frequency evolutions taken during a slow ($f_M = 0.04$ Hz) sinusoidal baseband modulation of the drive frequency $f_{dr}(t) = f_i + 2f_\Delta sin^2 \pi f_M t$ around the $k_z = 3$ *TG* mode frequency domain. Here, the initial (base) drive frequency $f_i = 5.5$ MHz, and the drive frequency deviation $f_\Delta =$ 0.1, 0.2, and 0.4 MHz.

In the case of fast drive frequency modulations, when $2\pi f_M \tau_c > 1$, the sawtooth-like oscillations of the plasma temperature are observed as shown on Fig. 5. The plasma temperature dynamics switches intermittently between sinusoidal heating and exponential cooling within the temperature range limited by the increased repetition rate.

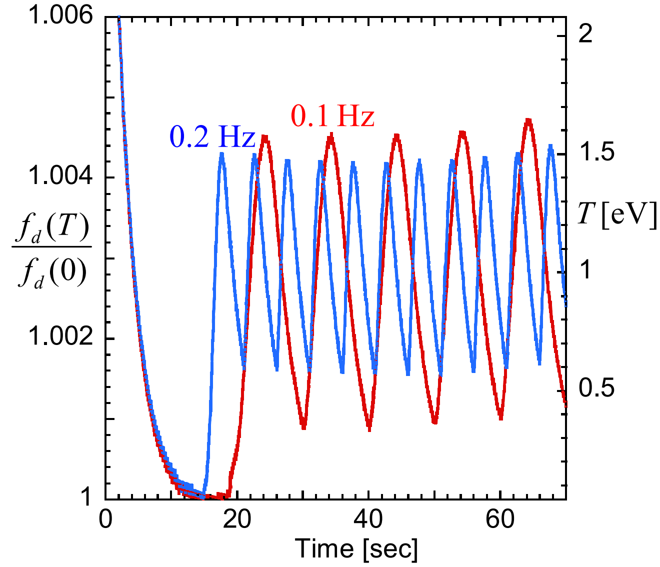

FIGURE 5. Plasma temperature and diocotron frequency evolutions taken during fast ($f_M = 0.1$ Hz, and $f_M = 0.2$ Hz) sinusoidal baseband modulation of the drive frequency $f_{dr}(t) = f_i + 2f_\Delta sin^2\pi f_M t$. Here, the initial (base) drive frequency $f_i = 5.4$ MHz, and the drive frequency deviation $f_\Delta = 0.3$ MHz.

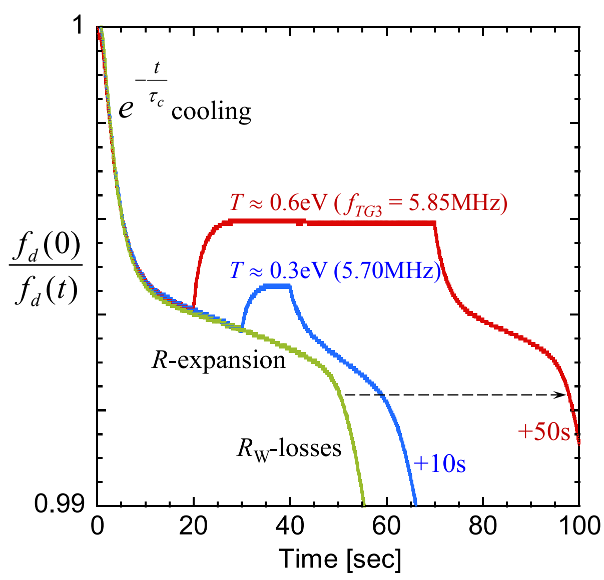

FIGURE 6. Diocotron frequency evolutions taken with and without frequency drives logarithmically swept to a desired $f_{TG}(T)$. Green: no drive applied. Red: a 5.85 MHz drive from $t = 20 \rightarrow 70$ sec pegs $T = 0.6$ eV. Blue: a 5.70 MHz drive from $t = 30 \rightarrow 40$ sec pegs $T = 0.3$ eV. Keeping the plasma temperature elevated delays the time when halo touches the wall (about at 50 sec with no temperature treatment, 60 sec and 100 sec for the evolutions with the elevated temperature phases).

Finally, we note that the plasma can be "pegged" to a fixed temperature for long times; but that the $f_d(T)$ diagnostic is perturbed by the formation and radial expansion of a low–density "halo" of particles at low temperatures ($T < 0.1$ eV). The electron temperature is "pegged" at a desired value (above the wall temperature) by applying a drive parked at the required TG mode frequency. Figure 6 shows the diocotron frequency evolution on a long time scale when no drive is applied. After an initial exponential drop, the diocotron frequency curve goes into a slow linear decline with time, associated with the low–density "halo" [2] radial expansion (the $R(t)$ term in Eq.1). When the cold plasma halo reaches the wall, the particle losses lead to a fast decline of the diocotron frequency. Application of the logarithmically swept frequency pulse (asymptoting to a chosen TG frequency value $f_{TG}(T)$) results into long lasting, autoresonantly locked frequency–temperature states. It is instructive to note that the very fact of keeping the plasma temperature above some critical level suspends the plasma halo expansion (very low radial transport) for the duration of the temperature treatment. For example, the 50 sec long pulse of the drive frequency keeps the plasma temperature at 0.6 eV and thus delays by 50 sec the time of halo touching the wall. This shows that the halo formation and its propagation to the wall are happening only in a cold enough plasma.

SUMMARY

This "at will" control of electron temperature may prove to be experimentally useful, especially for a variety of temperature sensitive processes like recombination, charge exchange and electron impact detachment in $e + H^-$ plasmas. Production and maintenance of negative hydrogen ions (H^-) with the binding energy of only 0.75 eV is a very tricky process in plasmas in general, but it seems that the tunable low temperature and long-lived electron plasma has unique properties to achieve significant progress in this delicate endeavor.

ACKNOWLEDGMENTS

This research was supported by the NSF/DoE partnership grants PHY-1414570 and DE-SC0002451, and by the DoE/HDELP grant DE-SC0008693.

REFERENCES

1. A. A. Kabantsev, Yu. A. Tsidulko, and C. F. Driscoll, Phys. Rev. Letters **112**, 055003 (2014).
2. A. A. Kabantsev, C. Y. Chim, T. M. O'Neil, and C. F. Driscoll, Phys. Rev. Letters **112**, 115003 (2014).
3. A. A. Kabantsev, D. H. E. Dubin, C. F. Driscoll, and Yu. A. Tsidulko, Phys. Rev. Letters **105**, 205001 (2010).
4. H. Higaki *et al*., Phys. Rev. E **65**, 046410 (2002).
5. M. D. Tinkle *et al*., Phys. Rev. Letters **72**, 352–355 (1994).
6. D. H. E. Dubin, Phys. Rev. Letters **66**, 2076–2079 (1991).
7. N. Shiga, F. Anderegg, D. H. E. Dubin, C. F. Driscoll, and R. W. Gould, Phys. Plasmas **13**, 022109 (2006).
8. F. Anderegg, N. Shiga, D. H. E. Dubin, C. F. Driscoll, and R. W. Gould, Phys. Plasmas **10**, 1556–1562 (2003).
9. K. S. Fine and C. F. Driscoll, Phys. Plasmas **5**, 601–607 (1998).
10. D. L. Eggleston *et al*., Phys. Fluids B **4**, 3432–3439 (1992).
11. R. C. Davidson, in *Physics of Nonneutral Plasmas* (Imperial College Press, London, 2001), pp. 249–253.